JACS
JOURNAL OF THE AMERICAN CHEMICAL SOCIETY
Article
pubs.acs.org/JACS

Pyrogallol[4]arenes as Frustrated Organic Solids

Harshita Kumari,[†] Loredana Erra,[‡] Alicia C. Webb,[†] Prashant Bhatt,[§] Charles L. Barnes,[†] Carol A. Deakyne,*[,†] John E. Adams,*[,†] Leonard J. Barbour,*[,§] and Jerry L. Atwood*[,†]

[†]Department of Chemistry, University of Missouri-Columbia, 601 S. College Avenue, Columbia, Missouri 65211, United States
[‡]European Synchrotron Radiation Facility, 8 Rue J. Horowitz, 38043 Grenoble, France
[§]Department of Chemistry, University of Stellenbosch, Private Bag X1, Matieland 7600, Stellenbosch, South Africa

Supporting Information

ABSTRACT: Two forms of interdigitated layered arrangements of *C*-pentylpyrogallol[4]arene (PgC_5) have been structurally elucidated and show variations in packing arrangements and host−guest interactions. Molecular dynamics simulations reveal a propensity for formation of self-included dimers, with or without incorporated solvent. Combined gas sorption and PXRD results show the presence of seven forms of PgC_5, with and without CO_2 (and their interconversions). This is the first CO_2 gas sorption study of pyrogallol[4]arenes, and it provides evidence that pyrogallol[4]arenes may act as frustrated organic solids.

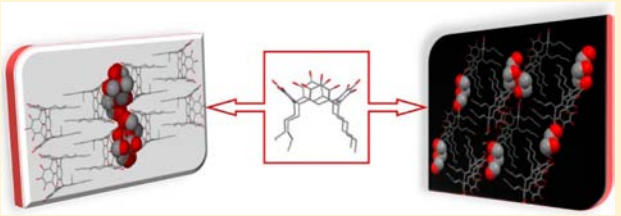

1. INTRODUCTION

Investigation of new materials for gas storage or separation is a significant area of endeavor. To date, nanoporous materials such as activated carbon,[1] carbon nanotubes,[2] zeolites,[3−5] and metal−organic frameworks[6] have served as excellent host assemblies with channels for gas sorption. In 2002, Atwood et al. discovered that *p*-tert-butylcalix[4]arene undergoes single-crystal-to-single-crystal phase transitions upon guest uptake and release.[7] This organic solid does not possess pores or channels in the solid state; however, guest transport through the solid occurs readily until a thermodynamically stable structure is achieved. For example, acetylene absorption in the seemingly nonporous, low-density polymorph of *p*-tert-butylcalix[4]arene is about 2% by weight, with a calculated density of the absorbed acetylene at STP of 90 times the compression limit for safe storage.[8] Several additional nonporous organic solids have also been found to exhibit remarkable sorption behavior.[4,5,9,10] These observations have led to identification of a new kind of porosity, transient porosity, typical of the so-called 'frustrated organic solids'.[11]

The current study focuses on the synthesis, packing arrangement, molecular dynamics, and gas sorption of *C*-pentylpyrogallol[4]arene (PgC_5). This is our first effort to exploit pyrogallol[4]arenes for gas sorption. These systems are of interest for gas sorption because our previous studies have demonstrated their ability to self-assemble into different architectures, such as bilayers, nanotubes, and nanocapsules, with solvent-accessible channels.[12−14] Differences in chain length and solvent have been shown to contribute to variations in packing arrangements and accessible void volumes. To avoid the multiplicity of possible chain orientations of long chains and/or the absence of hydrophobic channels in short chains, we selected the *C*-pentyl group for the first gas sorption studies. PgC_5 offers the possibility of examining the contributions of binding in hydrophobic and hydrophilic regions within the same material.

2. RESULTS AND ANALYSIS OF RESULTS

2.1. Dynamics Studies. To investigate the intrinsic relative orientations of PgC_5 molecules, we carried out molecular dynamics (MD) simulations, the specifics of which are given in the Supporting Information. As a preface to the examination of PgC_5 dynamics, we investigated the dynamics of the simpler PgC_0 species, i.e., the pyrogallol[4]arene macrocycle having no alkyl side chains. Specifically, we evaluated the structural stability of the PgC_0 dimeric hydrogen-bonded capsule and the propensity for the capsule to collapse to a self-inclusion complex. As shown in Figure 1, two types of self-inclusion complexes are possible. In the first type, which we will term "unilateral", a pyrogallol moiety of one macrocycle inserts itself into the cavity of the second macrocycle. In the second type, which we will term "bilateral", the second macrocycle also inserts one of its pyrogallols into the cavity of the first macrocycle, thereby yielding macrocycles that lie in interlaced parallel sheets. The gas-phase dimeric capsule at room temperature indeed is found to survive on the nanosecond time scale, with a free energy of binding of the macrocycles (from a potential of mean force calculation) of 74.0 ± 0.1 kJ mol^{-1}, essentially equivalent to the net strength of four hydrogen bonds. Because disruption of these hydrogen-bonding interactions might result from the presence of a polar guest, we also considered the stability of a capsule containing a single methanol molecule. The integrity of this gas-phase capsule is lost over the simulation time, with the PgC_0 macrocycles first forming a unilateral self-inclusion

Received: June 30, 2013
Published: September 16, 2013

   dx.doi.org/10.1021/ja406643b | *J. Am. Chem. Soc.* 2013, 135, 16963−16967

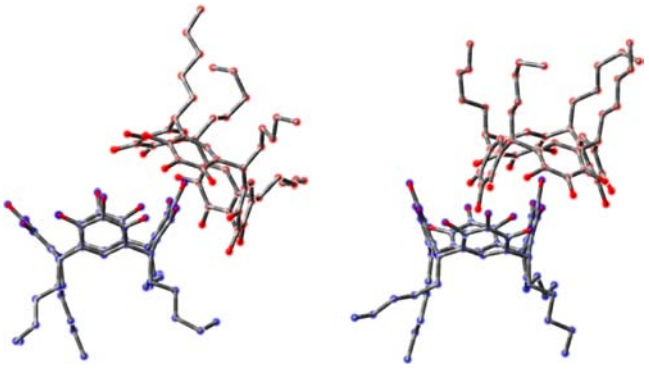

Figure 1. Representations of self-included PgC_5 dimers: unilateral (left) and bilateral (right). The atoms have been highlighted in red or blue to distinguish between the two macrocycles. The tilted relative orientation of the macrocycles' lower rims is characteristic of unilateral self-inclusion (left). O: red, C: gray, H: not shown.

complex in which the methanol molecule remains bound in one of the cavities and then eventually moving to a bilateral complex as the methanol molecule migrates to an exo binding position. This result suggests that in the gas phase, the extra stability of the bilateral self-inclusion complex offsets any loss of binding energy of the guest.

The different behaviors noted with and without the presence of a methanol guest motivated a consideration of capsule stability in polar methanol and less polar (and non-hydrogen-bonding) chloroform solvents. As anticipated, methanol does destabilize the capsule, not by simply separating and independently solvating the macrocycles but by promoting the formation of a self-inclusion complex. (Both the unilateral and bilateral structures are visited as time evolves. Note that the two structural types are easily distinguished by the relative orientations of the macrocycles' lower rims: they are tilted with respect on one another in the case of the unilateral structure but are parallel in the case of the bilateral structure.) However, the capsule−chloroform interactions are sufficiently weak that the solvated dimeric capsule survives for the entire simulation period. Given these different behaviors, one naturally wonders whether it is the polarity per se of the methanol that lies at the root of the difference or whether specific hydrogen bonding yields the observed effects. A simulation of the capsule solvated by dimethyl sulfoxide, which is more polar than methanol but is a poor hydrogen-bonding solvent, yields a structure in which the PgC_0 bowls are essentially nested, suggesting that solvent polarity ultimately destabilizes the dimeric capsule structure.

In turning to the PgC_5 macrocycle that is the focus of the present work, we find that the gas-phase dimeric capsule is stable only for a few hundred picoseconds, after which it converts to a bilateral self-inclusion complex. Inasmuch as the hydrogen-bonding interaction between the upper rims of the two macrocycles is expected to differ little from that in the PgC_0 dimer, the difference in the capsule dynamics must derive from the presence of the pentyl side chains. As the thermal energy of these side chains flows throughout the macrocycles, energy occasionally passes into a shearing mode whereby the two PgC_5 bowls translate in opposite directions. The complex then has sufficient energy in the appropriate mode to disrupt the intermolecular hydrogen bonds and to pass to the lower-energy self-inclusion structure, a structure that is sufficiently stable that the capsule structure is not subsequently revisited. This stability assessment was repeated with a methanol molecule equilibrated in the dimeric capsule, but as one would anticipate on the basis of the result found for the PgC_0 analog, the capsule does not survive intact in a 500 ps simulation. At the end of this simulation, a unilateral self-inclusion structure is found, with the methanol molecule occupying one of the cavities, thereby inhibiting formation of the bilateral structure. Comparison with our PgC_0 results suggests that this unilateral structure is likely to convert to the bilateral form with exo bound methanol at longer times.

Solvation of the PgC_5 dimeric capsule in either methanol or chloroform leads to disruption of the capsule. This observation is entirely consistent with the analysis of the gas-phase capsule given above, that thermal energy in the molecule is sufficient to overcome the energy barrier to formation of the self-inclusion complex. If we begin a simulation of the methanol-solvated capsule with an endo methanol guest, the disruption of the capsule does not displace the guest (the macrocycles form the unilateral complex with the bound guest residing in the PgC_5 that "donates" a pyrogallol moiety to the cavity of the other macrocycle), nor do we observe exchange of this methanol with bulk species on a nanosecond time scale.

In summary, the MD simulations predict a preference for a bilateral self-included complex or a unilateral complex with endo solvent. Of course, these predictions are made in the absence of any consideration of solid-state packing forces, and no provision is made for an interdigitation of the alkyl chains that might facilitate layering. The simulations nonetheless suggest structural motifs that could play an important role in determining crystal structures.

2.2. Experimental Studies. Crystals suitable for X-ray diffraction studies were obtained by slow evaporation of a methanolic solution of PgC_5. Prolonged standing and slow crystallization aided in formation of two different forms of crystals: needles (form I) and plates (form II).

Form I crystallizes in the triclinic space group *P*-1. The asymmetric unit (ASU) consists of one bowl of PgC_5 and three external methanol molecules located in the channel separating two adjacent PgC_5 bowls (Figure 2). The distances between the methanol and pyrogallol oxygen atoms range from 2.73 to 3.37 Å, indicating hydrogen-bonded interactions between these moieties on the basis of the criteria recommended for supramolecular and biochemical systems.[15−17] Two of the methanols H-bond to the central −OH and an outer −OH on the same pyrogallol. The third methanol interacts with the corresponding −OH groups on an adjacent pyrogallol of the same arene. One of the former methanol molecules also connects diagonally positioned macrocyles by forming H-bonds to outer −OH groups on different pyrogallols of the second arene. Individual arenes have a pinched cone arrangement with C···C distances of 6.56 and 9.98 Å. (These distances are measured between the carbons bonded to the central hydroxyls of opposing pyrogallols.) Despite the pinched arrangement, the O···O distances between adjacent pyrogallols in a given arene range from 2.83 to 3.17 Å, indicating persistence from the monomer to the dimer of an intramolecular H-bonded ring at the upper rim of the bowl.

Form II crystallizes in the monoclinic space group $P2_1/c$. The ASU consists of one PgC_5, one water, and three methanol molecules (Figure 2). The water molecule and two of the methanol molecules are outside the upper rim of the PgC_5 bowl, and the remaining methanol is enclosed as a guest within the bowl. The endo methanol is positioned with the methyl group facing toward the lower rim of the host macrocyle. The

dx.doi.org/10.1021/ja406643b | J. Am. Chem. Soc. 2013, 135, 16963−16967

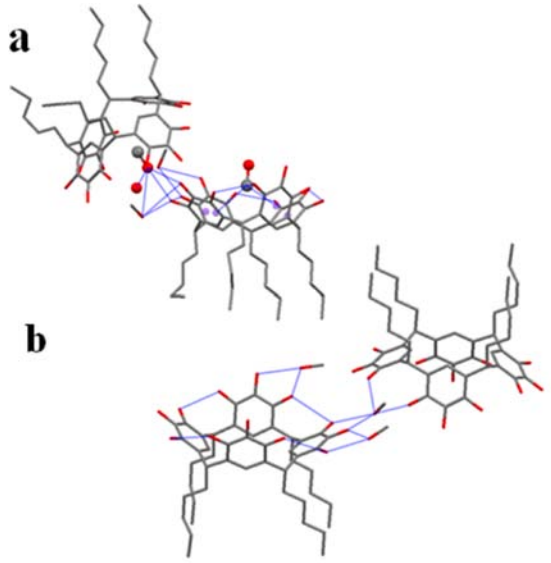

Figure 2. Single-crystal X-ray diffraction structure for *C*-pentylpyrogallol[4]arene form I/needle (a) showing one water and three methanol molecules. The endo methanol and exo water molecules are shown in ball and stick form and (b) showing three methanol molecules and form II/plate. Selected possible inter- and intramolecular H-bonding interactions discussed in the text are designated with dashed blue lines. The blue dots indicate ring centroids. For clarity hydrogen atoms and solvent molecules have been removed. O: red, C: gray.

−OH group of the enclosed methanol lies too far above the upper rim of the bowl to form O−H···O interactions with the host. However, the −OH group of this endo methanol interacts with two of the hydroxyls of a diagonally positioned arene with O···O distances of 2.84 and 2.85 Å. The endo methanol also interacts with an exo water (O···O distance: 2.68 Å) that is bridged between the two bowls (H_2O-to-diagonal-Pg O···O distance: 2.93 Å). The water also connects (a) the endo methanol to an exo methanol of the diagonally positioned arene with a H_2O-to-exo-MeOH O···O distance of 2.76 Å, (b) two diagonally positioned arenes through a central and an outer hydroxyl group with H_2O-to-Pg O···O distances of 2.71 and 2.93 Å, and (c) two adjacent arenes through their outer hydroxyl groups with H_2O-to-Pg O···O distances of 2.72 and 3.31 Å. These interactions also help explain the 1:1 ratio between the endo methanol and exo water in the ASU. The stability of the endo methanol is also enhanced by CH···π interactions with the nearest aryl rings; the C···centroid distances are 3.48 and 3.68 Å.

Each exo methanol of form II exhibits two O−H···O hydrogen bonds with the PgC_5 hydroxyl groups (O···O distances: 2.67 and 3.27; 2.78 and 3.40 Å). The two methanols interact with adjacent pyrogallols of the same arene. In each case the H-bonds involve the central and an outer hydroxyl of the pyrogallol. Although the arenes again have a pinched cone arrangement in form II, the pinching is not as severe as for the arenes of form I. The C···C distances between opposing pyrogallols for form II are 7.52 and 9.23 Å. Consistent with the more symmetric arrangement of the pyrogallols, the O···O distances in the intramolecular H-bonded ring of form II are shorter, ranging from 2.70 to 2.82 Å.

Symmetry expansion of the asymmetric units of form I (needles) and form II (plates) affords layered networks with solvent inclusion sites (Figure 3 and Supporting Information). The extended structures also reveal interdigitation between the

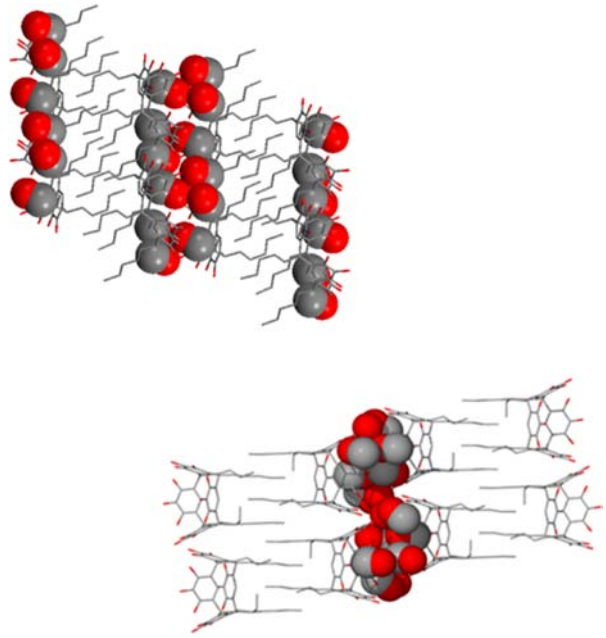

Figure 3. Packing diagrams of interdigitated heads and tails of self-included dimers of form I of PgC_5 with solvent (three methanols) inclusion between alternate dimers (top). Packing arrangement with interdigitated tails of form II of PgC_5 and heads showing channels of solvent inclusion (bottom).

'lower rim' *C*-pentyl chains of the pyrogallols, which maximizes the van der Waals interactions in a fashion typical for bilayer arrangements.[18] For form I, the layered network consists of closely packed bilateral self-included dimers whose tails are interdigitated with the adjacent layers, a structure consistent with the predictions derived from the MD simulations. With the enclosed methanol guest, the arenes in form II instead occupy offset positions. The location of the water of crystallization in form II is similar to that of the water molecule in the structure of PgC_5-MeCN·H_2O[18] and to that of the Cs ions in the structure of CsCl·PgC_4Cl.[19] Both the water and Cs^+ serve as a bridge between adjacent arenes. Here the observed endo methanol binding environment differs from that seen in the MD simulations, the difference likely being attributable to the use of a mixed solvent system in the experiments and to the exclusion in the simulations of any influences arising from ordering of the alkyl chains.

Space filling representations of forms I and II show solvent-occupied volumes of 13.6% and 6.6%, respectively. (Packing index calculations and Hirshfeld surface analyses can be found in the Supporting Information.) The available volumes suggested the possibility of gas−solvent exchange, which led us to perform a series of gas sorption and powder X-ray diffraction (PXRD) studies. A bulk crystalline sample of PgC_5 with included methanol (forms I and II) was exposed to CO_2 at 27 atm/RT to test for gas uptake. This solvated mixture sorbed only 1.5 wt % CO_2, and the PXRD of the CO_2 treated mixture indicates that a new form III is obtained (Figures 4 and 5). As the solvated forms were poor candidates for CO_2 sorption, we investigated desolvated and partially desolvated forms. We used dry versus wet methanol to obtain pure needles (form I) versus pure plates (form II) during the resynthesis process. Separate

dx.doi.org/10.1021/ja406643b | *J. Am. Chem. Soc.* 2013, 135, 16963−16967

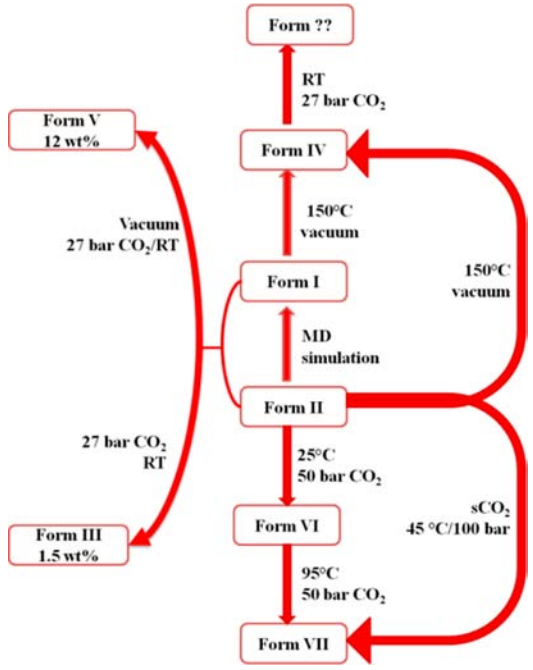

Figure 4. Flowchart of interconversions observed among the various forms of PgC_5 with and without CO_2.

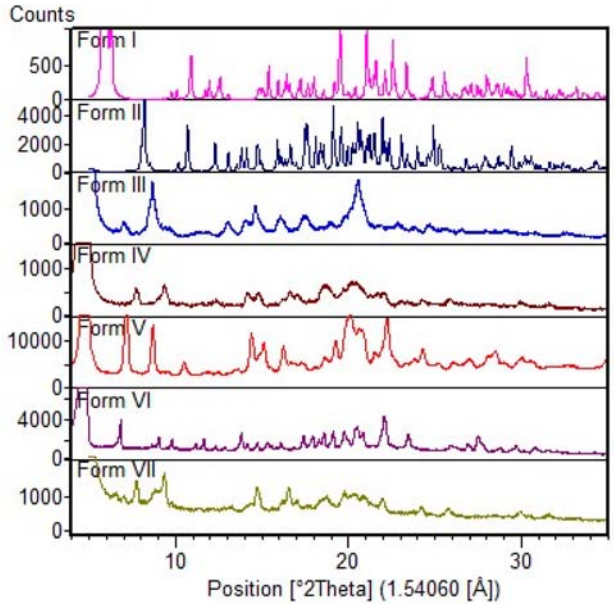

Figure 5. PXRD curve from top to bottom: forms I (magenta), II (navy), III (blue), IV (brown), V (red), VI (purple), and VII (olive).

sublimation/heat treatment of forms I and II at 150 °C for 8 h under vacuum led, in each case, to the formation of a new form IV, confirmed by PXRD (Figures 4 and 5). The gas sorption study of heat-treated form IV shows that the new form sorbs ~1.1 wt % CO_2 at 27 atm and RT.

In contrast, under milder treatment conditions (vacuum/RT for 6 h), the amount of CO_2 sorbed by a mixture of forms I and II is much higher (~12 wt %) than that sorbed by the heat-treated form IV (Figure 5). This result suggests that the milder conditions lead to a frustrated organic solid (form V) with partial solvent occupancies that prevent the framework from collapsing, facilitating passage of CO_2 into the framework (Figures 4 and 5). However, the heat-treated form IV likely has a more collapsed framework with fewer sites available for CO_2 sorption even under high pressure/RT conditions.

Finally, we performed capillary variable-temperature PXRD and supercritical CO_2 (sCO_2) experiments on form II. For the former experiment, crystals of form II were placed in a capillary which was subjected to 50 bar CO_2 and then sealed. The PXRD of the 50 bar/25 °C treated sample is different from that of form II indicating the presence of a new form VI (Figures 4 and 5). Varying the temperature from 25 to 210 °C, in increments of 10 °C, and concurrent PXRD measurements revealed a gradual transition from form VI to a new form VII in the vicinity of 95 °C. Interestingly, a differential scanning calorimeter (DSC) curve for form II demonstrates distinct solvent loss at ~85 and ~95 °C (Supporting Information). The presence of two peaks in the DSC curve can be attributed to the loss of water and methanol, perhaps the H-bonded pair, or to the loss of the endo methanol and an exo solvent molecule. In the sCO_2 experiment, a crystalline sample of form II was placed in an enclosed sCO_2 chamber at 100 bar/45 °C for 24 h. PXRD of this sample before and after treatment with sCO_2 revealed conversion of form II to VII (Figures 4 and 5). From these experiments one can infer that the same gradual phase change occurs both under conditions of 50 bar/95 °C CO_2 in a sealed capillary and at 100 bar/45 °C sCO_2 in a pressure chamber.

3. CONCLUSION

In conclusion, this work is the first reported study of the gas sorption properties of pyrogallol[4]arenes. We present the synthesis and structural elucidation of two crystalline bilayer inclusion complexes (forms I and II) of PgC_5, their characterizations being informed by gas- and solution-phase MD simulations. These complexes were subsequently subjected to a variety of gas sorption (sCO_2, variable temperature, sorption isotherms) and PXRD experiments from which we obtained five additional stable forms of PgC_5, with and without CO_2. Notably, the partially solvated form of PgC_5 (vacuum/RT treated) sorbs a much higher amount of CO_2 (12 wt %, form V) than the solvated (no treatment) and desolvated (150 °C/RT treated) forms (<1.6 wt %). These observations suggest that the PgC_5 exposed to vacuum is a partially desolvated structure/frustrated organic solid, thereby introducing pyrogallol[4]arenes as a new class of compounds having transient porosity.

■ ASSOCIATED CONTENT

Ⓢ Supporting Information

Simulation protocol, Hirshfeld surface analyses, gas sorption, PXRD and DSC curves, cif files. This material is available free of charge via the Internet at http://pubs.acs.org.

■ AUTHOR INFORMATION

Corresponding Authors

AtwoodJ@missouri.edu
AdamsJE@missouri.edu
DeakyneC@missouri.edu
ljb@sun.ac.za

Author Contributions

The manuscript was written with contributions from all authors. All authors have given approval to the final version of the manuscript.

Notes

The authors declare no competing financial interest.

■ ACKNOWLEDGMENTS

We thank National Science Foundation (JLA), the National Research Foundation (LJB), the Claude Leon Foundation (PB) and RSC Journals Grant for International Authors (HK) for financial support. We thank Agnieszka Janiak for help with the Crystal Explorer software.

■ REFERENCES

(1) Menon, V. C.; Komarneni, S. *J. Porous Mater.* **1998**, *5*, 43.
(2) Dillon, A. C.; Jones, K. M.; Bekkedahl, T. A.; Kiang, C. H.; Bethune, D. S.; Heben, M. J. *Nature* **1997**, *386*, 377.
(3) Corma, A. *Chem. Rev.* **1997**, *97*, 2373.
(4) Tedesco, C.; Erra, L.; Brunelli, M.; Cipolletti, V.; Gaeta, C.; Fitch, A. N.; Atwood, J. L.; Neri, P. *Chem.—Eur. J.* **2010**, *16*, 2371.
(5) Erra, L.; Tedesco, C.; Cipolletti, V. R.; Annunziata, L.; Gaeta, C.; Brunelli, M.; Fitch, A. N.; Knöfel, C.; Llewellyn, P. L.; Atwood, J. L.; Neri, P. *Phys. Chem. Chem. Phys.* **2012**, *14*, 311.
(6) Yaghi, O. M.; O'Keeffe, M.; Ockwig, N. W.; Chae, H. K.; Eddaoudi, M.; Kim, J. *Nature* **2003**, *423*, 705.
(7) Atwood, J. L.; Barbour, L. J.; Jerga, A.; Schottel, B. L. *Science* **2002**, *298*, 1000.
(8) Thallapally, P. K.; Dobrzańska, L.; Gingrich, T. R.; Wirsig, T. B.; Barbour, L. J.; Atwood, J. L. *Angew. Chem., Int. Ed.* **2006**, *45*, 6506.
(9) Thallapally, P. K.; Dalgarno, S. J.; Atwood, J. L. *J. Am. Chem. Soc.* **2006**, *128*, 15060.
(10) Dalgarno, S. J.; Thallapally, P. K.; Tian, J.; Atwood, J. L. *New J. Chem.* **2008**, *32*, 2095.
(11) Barbour, L. J. *Chem. Commun.* **2006**, 1163.
(12) Dalgarno, S. J.; Power, N. P.; Atwood, J. L. *Coord. Chem. Rev.* **2008**, *252*, 825.
(13) Jin, P.; Dalgarno, S. J.; Atwood, J. L. *Coord. Chem. Rev.* **2010**, *254*, 1760.
(14) Kumari, H.; Mossine, A. V.; Kline, S. R.; Dennis, C. L.; Fowler, D. A.; Teat, S. J.; Barnes, C. L.; Deakyne, C. A.; Atwood, J. L. *Angew. Chem., Int. Ed.* **2012**, *51*, 1452.
(15) McDonald, I. K.; Thornton, J. M. *J. Mol. Biol.* **1994**, *238*, 777.
(16) 27 Torshin, I. Y.; Weber, I. T.; Harrison, R. W. *Protein Eng. Des. Sel.* **2002**, *15*, 359.
(17) Steiner, G. R. D. T. *The Weak Hydrogen Bond: Applications to Structural Chemistry and Biology*; Oxford University Press: New York, 1999.
(18) Dalgarno, S. J.; Antesberger, J.; McKinlay, R. M.; Atwood, J. L. *Chem.—Eur. J.* **2007**, *13*, 8248.
(19) Dalgarno, S. J.; Power, N. P.; Atwood, J. L. *Chem. Commun.* **2007**, 3447.